*Tellus (2002), 54A, 363–369*
*Printed in UK. All rights reserved*


**TELLUS**
*ISSN 0280–6495*

# States of maximum entropy production in a one-dimensional vertical model with convective adjustment

By TONI PUJOL* and JOAQUIM FORT, *Departament de Física, Universitat de Girona, Campus Montilivi 17071, Girona, Catalonia, Spain*

(Manuscript received 1 October 2001; in final form 20 January 2002)

ABSTRACT

We investigate the hypothesis that the atmosphere is constrained to maximize its entropy production by using a one-dimensional (1-D) vertical model. We prescribe the lapse rate in the convective layer as that of the standard troposphere. The assumption that convection sustains a critical lapse rate was absent in previous studies, which focused on the vertical distribution of climatic variables, since such a convective adjustment reduces the degrees of freedom of the system and may prevent the application of the maximum entropy production (MEP) principle. This is not the case in the radiative–convective model (RCM) developed here, since we accept a discontinuity of temperatures at the surface similar to that adopted in many RCMs.

For current conditions, the MEP state gives a difference between the ground temperature and the air temperature at the surface $\approx 10$ K. In comparison, conventional RCMs obtain a discontinuity $\approx 2$ K only. However, the surface boundary layer velocity in the MEP state appears reasonable ($\approx 3$ m s$^{-1}$). Moreover, although the convective flux at the surface in MEP states is almost uniform in optically thick atmospheres, it reaches a maximum value for an optical thickness similar to current conditions. This additional result may support the maximum convection hypothesis suggested by Paltridge (1978).

## 1. Introduction

Recent theoretical analyses (Paltridge, 2001; Ozawa et al., 2001) support the hypothesis, first suggested by Lorenz (1960), that the atmosphere may be constrained to operate at its maximum thermodynamic efficiency. Since empirical support for this hypothesis, usually expressed as a maximum entropy production (MEP) principle, is based on the success of its application, several authors have examined the MEP principle in different climate models. A number of investigators have primarily addressed the latitudinal distribution of the main climatic variables by using climate models with very simplified vertical structures (e.g., Paltridge, 1975; Pujol et al., 1999). However, the turbulent flow, which is subject to the MEP requirement, plays a key role in defining the vertical atmospheric structure. Therefore, the proper reproduction of the vertical profile by the MEP principle applied to a vertical model is of great interest.

Pioneering studies focused on the vertical distribution by using highly idealized vertical models (e.g., Schulman, 1977; Shutts, 1981). Recently, Ozawa and Ohmura (1997) and Pujol (personal communication) have applied the MEP principle to comprehensive one-dimensional radiative–convective models (1-D RCMs) with similar results, although both studies use different methods [turbulent flux parameterized by eddy diffusion in Pujol (personal communication) and kept as an independent variable in Ozawa and Ohmura (1997)]. In essence, these authors find tropospheric temperature profiles that are con-

* Corresponding author.
e-mail: toni.pujol@udg.es

vectively unstable in the lower atmospheric levels and convectively stable in the upper ones. Such a temperature profile is similar to the distribution expected before using the convective adjustment, since the final result of convection is to sustain a critical lapse rate throughout the convective layer (Petterssen, 1940).

Differing with previous studies, here we prescribe the lapse rate in the convective layer and apply the MEP principle to the simple 1-D RCMs described in Section 2. Results are shown in Section 3, where the MEP states are compared with globally averaged data for current conditions on Earth and with outputs from conventional RCMs. Finally, the main conclusions from the present study are presented in Section 4.

## 2. The radiative–convective model

For simplicity, we assume a cloudless plane-parallel atmosphere and neglect scattering effects. In addition, we also assume the absorption of sunlight and infrared radiation independent of the respective short and long wavelengths. In other words, in our model the gray approximation holds in the corresponding spectral regions, albeit with different values of the absorption coefficient. The atmosphere is divided into two regions. The upper layer is in radiative equilibrium only (stratosphere), whereas the lower layer is in radiative–convective equilibrium (troposphere). The transition level between both layers is referred to as the tropopause.

### 2.1. Long-wave energy flux

In our model, infrared fluxes are described by Eddington's approximation, which simplifies the angular dependence of the specific intensity of radiation (Goody and Yung, 1989). Then, variations of the long-wave energy flux $F_{\mathrm{LW}}$ and globally averaged specific intensity of radiation $J$ through an atmospheric slab of optical thickness $\mathrm{d}\tau$ follow

$$\frac{\mathrm{d}F_{\mathrm{LW}}}{\mathrm{d}\tau} = 4(\pi J - \pi B), \tag{1a}$$

$$\frac{\mathrm{d}J}{\mathrm{d}\tau} = \frac{3}{4\pi} F_{\mathrm{LW}}, \tag{1b}$$

where $\tau$ is the infrared optical depth and $B$ is the integral over frequencies of the Planck function ($\pi B = \sigma T^4$, with $\sigma$ the Stefan–Boltzmann constant and $T$ the temperature).

We assume that the optical depth $\tau$ varies with height $z$ as (Weaver and Ramanathan, 1995)

$$\tau = \tau^* \, \mathrm{e}^{-z/H}, \tag{2}$$

where $\tau^*$ is the optical thickness of the whole atmosphere [$=\tau(z=0)$] and $H$ is the scale height of the absorbing gas ($\approx 2 \times 10^3$ m for water vapor).

### 2.2. Short-wave energy flux

Beer's law of absorption is applied to the short-wave energy flux $F_{\mathrm{sw}}$ (Ozawa and Ohmura, 1997)

$$F_{\mathrm{sw}} = F_{\mathrm{sw}}(0) \, \mathrm{e}^{-t}, \tag{3}$$

where $t$ is the short-wave optical depth and $F_{\mathrm{sw}}(0)$ is the net short-wave energy flux at top of the atmosphere (TOA) (i.e., at $t=0$). Since water vapor is the main absorber of sunlight (see Thomas and Stamnes, 1999), we may express $t$ as a linear function of $\tau$ (i.e., $t = \alpha\tau$, with $\alpha$ a constant). Ozawa and Ohmura (1997) suggest $\alpha = 0.53/\tau^*$ from comparison of eq. (3) with globally averaged data for current conditions on Earth.

### 2.3. Convective adjustment

We assume that convective processes in the troposphere sustain a prescribed lapse rate $\Gamma$ ($=-\mathrm{d}T/\mathrm{d}z$). From eq. (2), the tropospheric temperature profile expressed in terms of $\tau$ reads

$$\frac{\mathrm{d}\tau}{\mathrm{d}\tau} = \frac{H\Gamma}{\tau}, \tag{4}$$

where $\Gamma$ is the environmental lapse rate ($= 6.5 \times 10^{-3}$ K m$^{-1}$). The convective adjustment here employed has been extensively used in modeling the vertical temperature profile, with the environmental lapse rate corresponding to the standard tropospheric value (see, e.g., Ramanathan and Coakley, 1978).

### 2.4. Entropy production

The total entropy production due to convective processes $P_{\mathrm{ev}}$ follows from Ozawa and Ohmura (1997)

$$P_{cv} = F_{cv}(\tau^*)\left(\frac{1}{T_g} - \frac{1}{T(\tau^*)}\right) + \int_{\tau^*}^{\tau_{tpp}} F_{cv}(\tau)\frac{d}{d\tau}\left(\frac{1}{T(\tau)}\right)d\tau, \quad (5)$$

where $F_{cv}(\tau)$ is the convective energy flux $[=F_{SW}(\tau) - F_{LW}(\tau)]$ and $\tau_{tpp}$ is the optical depth of the tropopause. In eq. (5), $T_g$ is the ground temperature that may differ from the air temperature at the surface $T(\tau^*)$. The difference between both temperatures may be used to obtain the convective energy flux at the surface $F_{cv}(\tau^*)$ from the bulk aerodynamic formula (e.g., Schulman, 1977; Lindzen et al., 1982)

$$F_{cv}(\tau^*) = C_D u^* \rho(\tau^*) c_p [T_g - T(\tau^*)], \quad (6)$$

where $C_D$ is the aerodynamic drag coefficient, $u^*$ is the surface boundary layer velocity, $\rho(\tau^*)$ is the air density at the surface and $c_p$ is the specific heat of dry air at constant pressure ($=1005\ \mathrm{J\ K^{-1}\ kg^{-1}}$). Notice that we assume dry convection only (latent heat is ignored). Equation (6) will be used to evaluate $u^*$ for different atmospheric profiles.

### 2.5. *Numerical procedure*

The condition of radiative equilibrium in the stratosphere implies $F_{SW}(\tau) = F_{LW}(\tau)$ for $0 \leqslant \tau \leqslant \tau_{tpp}$, so from eq. (3) and the text below it

$$F_{LW}(\tau) = F_{SW}(0)\ e^{-\alpha\tau}. \quad (7)$$

Equation (7) is substituted in the right-hand side of eq. (1b), and the equation is integrated from TOA ($\tau = 0$) to the tropopause ($\tau = \tau_{tpp}$) using the boundary condition of zero downward long-wave flux at TOA [equivalent to $F_{LW}(0) = 2\pi J(0)$]. The final result is

$$\pi J(\tau) = F_{SW}(0)\left(\frac{1}{2} + \frac{3}{4\alpha}(1 - e^{-\alpha\tau})\right). \quad (8)$$

Equations (7) and (8) are used in eq. (1a), leading to

$$\sigma T(\tau)^4 = F_{SW}(0)\left(\frac{1}{2} + \frac{3}{4\alpha}(1 - e^{-\alpha\tau}) + \frac{\alpha}{4}e^{-\alpha\tau}\right). \quad (9)$$

For fixed values of $F_{SW}(0)$ and $\tau^*$, we choose an arbitrary value of $\tau_{tpp}$ ($0 < \tau_{tpp} < \tau^*$). Values of $F_{LW}$, $J$ and $T$ at $\tau = \tau_{tpp}$ are obtained from eqs. (7)–(9). These values are taken as initial points in the integration from $\tau = \tau_{tpp}$ to $\tau = \tau^*$ of the set of three ordinary differential equations (ODEs) formed by eqs. (1a and b) and (4). The ground temperature $T_g$ is obtained from the boundary condition at the surface that requires an upward long-wave emission at the surface equal to $\sigma T_g^4$ [i.e., $\sigma T_g^4 = \pi J(\tau^*) + F_{LW}(\tau^*)/2$]. The integration of the last term in the right-hand side of eq. (5) is also performed, and the numerical process uses a Runge–Kutta method with adaptive step-size (Press et al., 1994).

## 3. Results and discussion

Globally averaged values for current Earth conditions suggest a net short-wave flux at TOA $F_{SW}(0)$ equal to 240 W m$^{-2}$ (Ozawa and Ohmura, 1997) and an optical thickness $\tau^*$ equal to 4 (Goody and Yung, 1989). Figure 1 shows the total entropy production due to convective processes $P_{cv}$ (solid line), the energy flux at the surface $F_{cv}(\tau^*)$ $[=F_{SW}(\tau^*) - F_{LW}(\tau^*)]$ (dashed line) and the surface boundary layer velocity $u^*$ (short-dashed line) as a function of the thermal discontinuity at the surface $[\Delta T(\tau^*) = T_g - T(\tau^*)]$. Different values

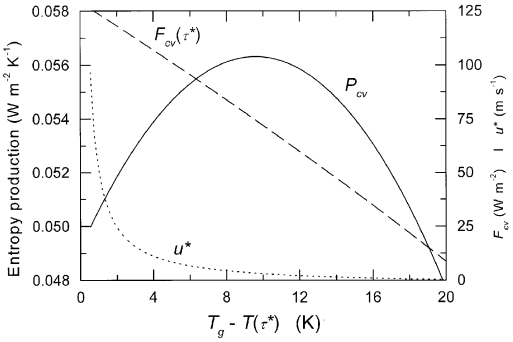


*Fig. 1.* Entropy production due to convective processes $P_{cv}$ (solid line; left vertical axis), convective flux at the surface $F_{cv}(\tau^*)$ (dashed line; right vertical axis), and boundary layer velocity $u^*$ (short-dashed line; right vertical axis) as a function of the discontinuity of temperatures at the surface $T_g - T(\tau^*)$. $T_g$ and $T(\tau^*)$ are the ground temperature and the air temperature at the surface, respectively. The net short-wave energy flux at TOA $F_{SW}(0)$ is 240 W m$^{-2}$ and the optical thickness $\tau^*$ is 4. With these conditions, the RCM with convective adjustment obtains a maximum value of $P_{cv}$ at $T_g - T(\tau^*) = 9.7$ K.

of $\Delta T(\tau^*)$ correspond to different values of the tropopause height $z_{tpp}$ (or, equivalently, $\tau_{tpp}$).

Results from the convective adjustment with continuity of temperatures at the surface [$\Delta T(\tau^*) = 0$] are obtained by using the value of $\tau_{tpp}$ such that it yields $\Delta T(\tau^*) = 0$. They give $T_g = T(\tau^*) = 281$ K, $F_{cv}(\tau^*) = 129$ W m$^{-2}$ and $P_{cv} = 0.0493$ W m$^{-2}$ K$^{-1}$. In this case, $F_{cv}(\tau^*)$ cannot be defined in terms of $u^*$ as in eq. (6). The MEP state in Fig. 1 (i.e., state of maximum $P_{cv}$) corresponds to $\Delta T(\tau^*) \approx 10$ K [with $T(\tau^*) = 281$ K], $F_{cv}(\tau^*) \approx 74$ W m$^{-2}$ and $P_{cv} \approx 0.0563$ W m$^{-2}$ K$^{-1}$. From eq. (6) and using $\rho(\tau^*) = 1$ kg m$^{-3}$ and $C_D = 0.0124$ m s$^{-1}$ (Lindzen et al., 1982) we find $u^* \approx 3$ m s$^{-1}$. In comparison, globally averaged Earth values are $T(\tau^*) = 288$ K and $F_{cv}(\tau^*) = 102$ W m$^{-2}$ (Ozawa and Ohmura, 1997). The estimation of the total non-radiative entropy production (including irreversible effects of condensation and evaporation here ignored) is $\approx 0.0325$ W m$^{-2}$ K$^{-1}$ (Goody, 2000). A mean estimate of the surface boundary layer velocity $u^*$ is $\approx 5$ m s$^{-1}$ (Lindzen et al., 1982).

MEP values of $T(\tau^*)$ and $F_{cv}(\tau^*)$ closer to globally averaged data may be obtained by using a smaller value of $\alpha$ [see the text below eq. (3)]. Here we assume that the atmosphere absorbs about 41% of the net short-wave radiation at TOA (Ozawa and Ohmura, 1997), while some authors adopt an absorption $\approx 30\%$ only (Thomas and Stamnes, 1999). In addition, the discontinuity of temperatures at the surface ($\approx 10$ K) is larger than that found in 'classical' RCMs ($\approx 2$ K; see Lindzen et al., 1982), although it agrees with some results obtained by Schulman (1977) in a simplified 2-D model at the maximum rate of energy dissipation. From the data shown above, the non-radiative entropy production $P_{cv}$ obtained from the model is larger than the expected value for current Earth conditions. However, its value is similar to results obtained from vertical climate models ($\approx 0.062$ W m$^{-2}$ K$^{-1}$ in Li et al., 1994; $\approx 0.054$ W m$^{-2}$ K$^{-1}$ in Ozawa and Ohmura, 1997).

In Fig. 1, $\tau^* = 4$ and then $z_{tpp}$ varies $\approx 6$ m from $\Delta T(\tau^*) = 0$ K ($z_{tpp} = 9318$ m) to $\Delta T(\tau^*) = 20$ K ($z_{tpp} = 9312$ m). In contrast, $z_{tpp}$ varies $\approx 1600$ m for the same range of variation of $\Delta T(\tau^*)$ in an atmosphere with optical thickness $\tau^* = 1$. Figure 2 shows the discontinuity of temperatures at the surface $\Delta T(\tau^*)$ as a function of the variation in the tropopause height $\Delta z_{tpp}$ for atmospheres with different opacities. Notice that the tropopause height decreases as $\Delta T(\tau^*)$ increases. Squares show the MEP states. From Fig. 2, the discontinuity of temperatures at the surface is seen to be very sensitive to changes in the tropopause height for optically thick atmospheres only. The greenhouse effect in these types of atmospheres is so intense that the downward long-wave flux at the surface almost balances the upward one when we assume a continuity of temperatures at the surface [i.e., $\Delta T(\tau^*) = 0$]. Then, and from the boundary condition at the surface [see the paragraph below eq. (9)], the surface value of the specific intensity of radiation $J(\tau^*)$ is very similar to Planck's function $B(\tau^*)$. When we assume a ground temperature $T_g$ different (and greater) than $T(\tau^*)$, the upward long-wave flux at the surface exceeds that of the $\Delta T(\tau^*) = 0$ case. This may lead to atmospheric regions (mainly near the surface) where $dF_{LW}/d\tau > 0$ [i.e., regions where $J > B$; see eq. (1a)]. In such cases, and since $F_{LW}$ and $J$ must be always positive, the right hand sides of eq. (1a and b) take positive values, so both $F_{LW}$ and $J$ may increase as a function of $\tau$ following an exponential-like dependence. It may be illustrative to point out that the analytical solution of $F_{LW}$ from eq. (1a and b) with the additional simplifica-

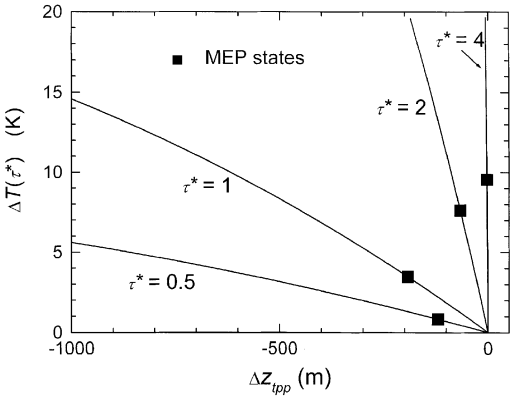


*Fig. 2.* Discontinuity of temperatures at the surface $\Delta T(\tau^*)$ as a function of the variation in the tropopause height $\Delta z_{tpp}$ for atmospheres with different opacities $\tau^*$. Squares show the MEP states. The tropopause heights for $\Delta T(\tau^*) = 0$ are: $z_{tpp}(\tau^* = 0.5) = 2044$ m, $z_{tpp}(\tau^* = 1) = 4856$ m, $z_{tpp}(\tau^* = 2) = 7299$ m, and $z_{tpp}(\tau^* = 4) = 9318$ m. The net short-wave energy flux at TOA $F_{SW}(0)$ is 240 W m$^{-2}$.

tions of an optical depth linear in height and a linear approximation of $B$ in temperature corresponds to a double exponential with positive and negative exponents. In this case, the two constants that multiply the double exponentials are obtained by applying the boundary conditions (7) and (8) to the tropopause. It turns out that, in optically thick atmospheres, these constants are very sensitive to the tropopause height because of the exponential-like dependence of $F_{LW}$ on $z$ (or, equivalently, on $\tau$). Then, small changes in $z_{tpp}$ may indeed lead to large changes in the values of $F_{LW}$ at the surface, and hence in the values of $T_g$. The high sensitivity of surface values to changes in tropopause heights for optically thick atmospheres has been already pointed out by Kasting et al. (1984) and Abe and Matsui (1988).

For the same value of the net short-wave flux at TOA as that used in Figs. 1 and 2 [$F_{SW}(0) = 240\ \mathrm{W\ m^{-2}}$], Fig. 3 plots the ground temperature $T_g$, the air temperature at the surface $T(\tau^*)$, the tropopause temperature $T_{tpp}$, and the TOA temperature $T_{toa}$ for the MEP states at a given optical thickness $\tau^*$. For comparison purposes, the ground temperature [from $\sigma T_g^4 = \pi J(\tau^*) + F_{LW}(\tau^*)/2$] and the air temperature at the surface [from eq. (9)] for atmospheres in radiative equilibrium [i.e., such that eqs. (8) and (9) hold for all the atmosphere] are also shown (dashed lines). Since the absorption is gray, $T_{toa}$ for the radiative equilibrium atmosphere coincides with the radiative–convective case, and its numerical value follows from eq. (9) with $\tau = 0$. Values for $\tau^* < 0.3$ are omitted since the atmospheric absorption of sunlight would imply values of $T_g$ lower than $T(\tau^*)$. This behavior is not observed for an atmosphere totally transparent to sunlight (i.e., with $\alpha = 0$). Figure 3 indicates that $T_g$ and $T(\tau^*)$ in MEP states increase monotonically with $\tau^*$, and their difference $\Delta T(\tau^*)$ asymptotically approaches $\approx$ 10 K. Results from applying the convective adjustment with the condition of continuity of temperatures at the surface (as, e.g., in Manabe and Strickler, 1964) are very similar to those obtained for the MEP states (solid lines in Fig. 3), except than in such a model one has $T_g = T(\tau^*)$.

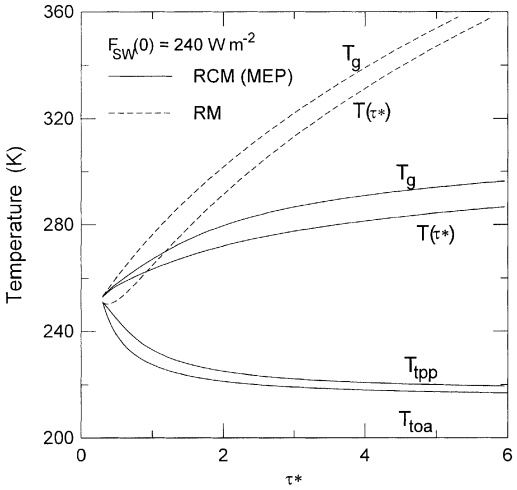


*Fig. 3.* Ground temperature $T_g$, air temperature at the surface $T(\tau^*)$, tropopause temperature $T_{tpp}$, and TOA temperature $T_{TOA}$ of the states that maximize $P_{cv}$ at each optical thickness $\tau^*$ (solid lines). For $\tau^* = 4$, the maximum entropy production (MEP) state corresponds to that with the maximum $P_{cv}$ observed in Fig. 1. We also include the ground temperature $T_g$, air temperature at the surface $T(\tau^*)$, and TOA temperature $T_{TOA}$ (coincides with the RCM value) of a pure radiative equilibrium model (dashed lines). The net short-wave energy flux at TOA $F_{SW}(0)$ is 240 W m$^{-2}$.

Finally, the convective flux at the surface $F_{cv}(\tau^*)$ for the MEP states of Fig. 3 is shown in Fig. 4. We also include the value of $F_{cv}(\tau^*)$ for a RCM with continuity of temperatures at the surface, since this condition is usually applied in RCMs. In the latter case, $F_{cv}(\tau^*)$ increases monotonically with $\tau^*$. In contrast, $F_{cv}(\tau^*)$ in optically thick ($\tau^* > 2$) MEP atmospheres is almost uniform, although a detailed analysis shows that $F_{cv}(\tau^*)$ reaches a maximum value of 74.4 W m$^{-2}$ at $\tau^* \approx 3.8$ (see the inset in Fig. 4). This value is very close to the optical thickness expected for current Earth conditions. Therefore, this result may give support to the convective hypothesis introduced by Paltridge (1978), who suggested that the Earth's climate is not only constrained to maximize its thermodynamic efficiency (Fig. 1) but also to maximize the convective flux at the surface (Fig. 4, inset). It is worth noting that Paltridge applies the maximum convective assumption to MEP states by finding the temperature that maximizes the convective heat flux at a constant optical thickness. In contrast, the maximum convective heat flux $F_{cv}(\tau^*)$ derived from Fig. 4 is the upper bound of $F_{cv}(\tau^*)$ determined by the MEP principle when varying the optical depth. Actually,

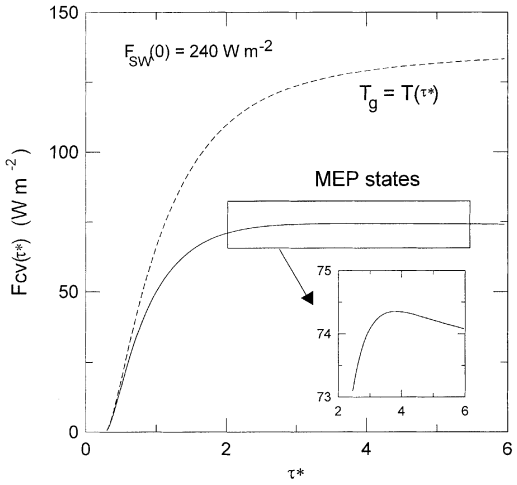


*Fig. 4.* Convective energy flux at the surface $F_{cv}(\tau^*)$ for the MEP states shown in Fig. 3 (solid line) and for a RCM with convective adjustment and continuity of temperatures at the surface (dashed line). The inset shows (at a different scale) the value of $F_{cv}(\tau^*)$ for optically thick MEP atmospheres in detail, where a maximum value of $F_{cv}(\tau^*)$ ($=74.4$ W m$^{-2}$) at $\tau^* = 3.8$ is found. The net short-wave energy flux at TOA $F_{SW}(0)$ is 240 W m$^{-2}$.

the large difference between $T_g$ and $T(\tau^*)$ found at the MEP states in optically thick atmospheres (Fig. 2) is the cause of the low values of $F_{cv}(\tau^*)$ found in Fig. 4 in comparison with the classical version of the convective adjustment [i.e., $T_g = T(\tau^*)$].

## 4. Conclusions

We have used a 1-D vertical model with convective adjustment to examine the hypothesis that the atmosphere operates at its maximum thermodynamic efficiency. We have expressed this hypothesis in terms of a MEP principle. The main difference with earlier 1-D vertical analyses of the MEP principle (see, e.g., Schulman, 1977; Ozawa and Ohmura, 1997) has been the assumption that convective processes sustain a critical lapse rate in the troposphere. This convective adjustment has been introduced in a very simple model with gray absorption in the short- and the long-wave spectrum. For fixed values of atmospheric opacity $\tau^*$ and net short-wave flux at TOA $F_{SW}(0)$, the entropy production is a function of the discontinuity of temperatures at the surface (Fig. 1). The state that maximizes the entropy production due to convective processes in an atmosphere with $\tau^* = 4$ and $F_{SW}(0) = 240$ W m$^{-2}$ (similar to current Earth's conditions) shows a discontinuity of temperatures at the surface $\approx 10$ K (air temperature at the surface equal to 281 K). In comparison, the conventional RCM developed by Lindzen et al. (1982) gives a difference of temperatures at the surface $\approx 2$ K and an air temperature at the surface $\approx 286$ K [although with $F_{SW}(0) = 274$ W m$^{-2}$]. The MEP state gives a reasonable surface boundary layer velocity ($\approx 3$ m s$^{-1}$) from the bulk aerodynamic formula. However, the discontinuity of temperatures at the surface at the MEP state seems too large, so the success of the MEP principle applied to the 1-D RCM with convective adjustment may be questionable.

If we accept the MEP principle, an intriguing result arises when examining different atmospheric opacities with the same external forcing [$F_{SW}(0) = 240$ W m$^{-2}$]. The convective flux in optically thick atmospheres is almost independent of $\tau^*$, and reaches a maximum value at $\tau^* = 3.8$ (Fig. 4, inset), which is very close to the expected value for current conditions on Earth. (A similar result is also obtained by using an atmosphere totally transparent to sunlight.) This result may suggest that among the MEP states, the atmosphere chooses that with maximum convection. This maximum convective hypothesis was first introduced by Paltridge (1978) and applied with the MEP principle in following versions of Paltridge's box-model (e.g., Gerard et al., 1990; O'Brien and Stephens, 1995; Pujol and Llebot, 2000a, b). Although the convective principle has often been ignored, O'Brien and Stephens (1995) showed the important role of this hypothesis in the results obtained from using Paltridge's box-model.

The present study adds a new model to the long list of climate models where the MEP principle has been applied. The enforcement of a prescribed lapse rate in the troposphere generates both good (e.g., $u^*$) and bad [e.g., $\Delta T(\tau^*)$] values of some important climatic parameters. Therefore additional studies are required in order to examine the implications of the MEP principle (and, also, of the convective hypothesis) in atmospheres with

convective adjustment. Of particular importance is the analysis of a more realistic non-gray RCM, which is expected to reduce the $\Delta T(\tau^*)$ (Manabe and Strickler, 1964), and this is the purpose of our continuing research.

## 5. Acknowledgements

This work has been partially funded by the Ministerio de Educación y Cultura of the Spanish Government under contract REN 2000-1621 CLI.

## REFERENCES

Abe, Y. and Matsui, T. 1988. Evolution of an impact-generated $H_2O$–$CO_2$ atmospere and formulation of a hot proto-ocean on Earth. *J. Atmos. Sci.* **45**, 3081–3101.

Gerard, J.-C., Delcourt, D. and Francois, L. M. 1990. The maximum entropy production principle in climate models: application to the faint young sun paradox. *Q. J. R. Meteorol. Soc.* **116**, 1123–1132.

Goody, R. 2000. Sources and sinks of climate entropy. *Q. J. R. Meteorol. Soc.* **126**, 1953–1970.

Goody, R. M. and Yung, Y. L. 1989. *Atmospheric radiation. Theoretical basis.* 2nd edn. Oxford University Press, New York, 519 pp.

Kasting, J. F., Pollack, J. B. and Ackerman, T. P. 1984. Response of Earth's atmosphere to increase in solar flux and implications for loss of water from Venus. *Icarus* **57**, 335–355.

Li, J., Chýlek, P. and Lesins, G. B. 1994. Entropy in climate models. Part I: Vertical structure of atmospheric entropy production. *J. Atmos. Sci.* **51**, 1691–1708.

Lindzen, R. S., Hou, A. Y. and Farrell, B. F. 1982. The role of convective model choice in calculating the climate impact of doubling $CO_2$. *J. Atmos. Sci.* **39**, 1189–1205.

Lorenz, E. N. 1960. Generation of available potential energy and the intensity of the general circulation. In *Dynamics of climate* (ed. R. L. Pfeffer). Pergamon Press, Oxford, pp. 86–92.

Manabe, S. and Strickler, R. F. 1964. Thermal equilibrium of the atmosphere with a convective adjustment. *J. Atmos. Sci.* **21**, 361–385.

O'Brien, D. M. and Stephens, G. L. 1995. Entropy and climate. II: Simple models. *Q. J. R. Meteorol. Soc.* **121**, 1773–1796.

Ozawa, H. and Ohmura, A. 1997. Thermodynamics of a global-mean state of the atmosphere — a state of maximum entropy increase. *J. Climate* **10**, 441–445.

Ozawa, H., Shimokawa, S. and Sakuma, H. 2001. Thermodynamics of fluid turbulence: a unified approach to the maximum transport properties. *Phys. Rev. E.* **64**, 026 303.

Paltridge, G. W. 1975. Global dynamics and climate — a system of minimum entropy exchange. *Q. J. R. Meteorol. Soc.* **101**, 475–484.

Paltridge, G. W. 1978. The steady-state format of global climate. *Q. J. R. Meteorol. Soc.* **104**, 927–945.

Paltridge, G. W. 2001. A physical basis for a maximum of thermodynamic dissipation of the climate system. *Q. J. R. Meteorol. Soc.* **127**, 305–313.

Petterssen, S. 1940. *Weather analysis and forecasting.* McGraw-Hill, New York, 505 pp.

Press, W. H., Teukolsky, S. A., Vetterling, W. T. and Flannery, B. P. 1994. *Numerical recipes in Fortran. The art of scientific computing*, 2nd edn. Cambridge University Press, New York, 963 pp.

Pujol, T. and Llebot, J. E. 2000a. Extremal climatic states simulated by a 2-dimensional model. Part I: Sensitivity of the model and present state. *Tellus* **52A**, 422–439.

Pujol, T. and Llebot, J. E. 2000b. Extremal climatic states simulated by a 2-dimensional model. Part II: Different climatic scenarios. *Tellus* **52A**, 440–454.

Pujol, T., Llebot, J. E. and Fort, J. 1999. Greenhouse gases and climatic states of minimum entropy production. *J. Geophys. Res.* **104**, D20, 24257–24263.

Ramanathan, V. and Coakley, J. A. Jr. 1978. Climate modeling through radiative–convective models. *Rev. Geophys. Space Phys.* **16**, 465–489.

Schulman, L. L. 1977. A theoretical study of the efficiency of the general circulation. *J. Atmos. Sci.* **34**, 559–579.

Shutts, G. J. 1981. Maximum entropy production states in quasi-geostrophic dynamical models. *Q. J. R. Meteorol. Soc.* **107**, 503–520.

Thomas, G. E. and Stamnes, K. 1999. *Radiative transfer in the atmosphere and ocean.* Cambridge University Press, Cambridge, 517 pp.

Weaver, C. P. and Ramanathan, V. 1995. Deduction from a simple climate model: factors governing surface temperature and atmospheric thermal structure. *J. Geophys. Res.* **100**, 11 585–11 591.